Table II. Reactions Not Exhibiting Oscillatory Gas Evolution

first reactant	second reactant	solvent[a]	gaseous product
N_2H_4	Fe^{3+}, H^+	C	N_2
H_2NCONH_2	OBr^-	C	N_2
$NaBH_4$	H^+	C	H_2
NaCl	H_2SO_4	A	HCl
CO_3^{2-}	H^+	C	CO_2
SO_3^{2-}	H^+	C	SO_2

[a] A ≡ concentrated H_2SO_4; C ≡ water.

bubbles present followed by a chain of oscillations that (in contrast to the organic acid reactions) produce almost no foam.

If anything, oscillations in the two nitrous acid reactions are more irreproducible than those for the organic acids. Not only are concentration, temperature, and agitation important, but also pH and the order in which the reactants are mixed. At the conditions given in Table I, we found that the most repeatable oscillations were produced by mixing $NaNO_2$ and H_2SO_4 solutions and allowing the resulting HNO_2 solution to equilibrate to bath temperature (with occasional agitation to remove most of the NO_2 fumes) before being added to the NH_4Cl or urea.

Other Reactions. We tried without success to generate oscillations with a number of other reactions known to produce gaseous products. Some of these failures are summarized in Table II. Of course we have shown not that oscillatory gas evolution is impossible for these systems but only that such behavior was not exhibited in our hands.

Discussion

The main fact we wish to establish in this paper is that gas evolution oscillations are of much more widespread occurrence than has previously been reported. It is at first sight surprising that some of the oscillations have not been seen previously, because the overall kinetics of the reactions has been known for some years. This is particularly true for oxalic, citric, and malic acids[10] and for the HNO_2 processes.[11,12]

We believe there are two reasons oscillations were missed in earlier studies. In the first place, the concentrations required for rhythmic gas evolution (see Table I) are much higher than those that for obvious reasons were employed in regular kinetic studies. In the second place, measurements of gas evolution rates (a usual method for monitoring the reactions) are generally done with vigorous agitation to *prevent* supersaturation; while the oscillations, as we are now convinced, occur as a result of the natural release of supersaturation.

This first paper is intended to be primarily phenomenological with our interpretations to follow. However, it should already be apparent that we believe nucleation and supersaturation processes are the major factors responsible for oscillatory behavior in many of these systems. We do not exclude the possibility that chemical processes may sometimes couple with gas evolution in order to cause or enhance oscillatory behavior. The best candidates for such coupling with chemical reactions are the reactions of ammonium ion and urea with nitrous acid and the sulfuric–nitric–formic acid system of Raw et al.[13]

Acknowledgment. Much of the experimental work was performed by P.G.B. at the University of Oregon while on leave from Simmons College. Some preliminary studies of the ammonium nitrite system were made by Dr. Kenneth W. Smith; we first learned of the oscillatory potential of this reaction from Professor H. Degn of the University of Odense.[14] The work was supported in part by a Grant from the National Science Foundation.

Registry No. NH_4Cl, 12125-02-9; NO_2^-, 14797-65-0; $C_6H_5N_2Cl$, 100-34-5; H_2SO_4, 7664-93-9; H_3PO_4, 7664-38-2; HNO_2, 7782-77-6; H_2O_2, 7722-84-1; N_2H_4, 302-01-2; $NaBH_4$, 16940-66-2; NaCl, 7647-14-5; CO_3^{2-}, 3812-32-6; SO_3^{2-}, 14265-45-3; Fe^{3+}, 20074-52-6; OBr^-, 14380-62-2; malic acid, 6915-15-7; oxalic acid, 144-62-7; tartaric acid, 87-69-4; citric acid, 77-92-9; malonic acid, 141-82-2; formic acid, 64-18-6; nitric acid, 7697-37-2; urea, 57-13-6.

(10) Liler, M. "Reaction Mechanisms in Sulfuric Acid"; Academic Press: New York, 1971.

(11) Werner, E. A. "The Chemistry of Urea"; Longmans, Green & Co.: London, 1923.

(12) Hughes, E. D.; Ingold, C. K.; Ridd, J. H. *J. Chem. Soc.* **1958**, 58–65, 65–69, 70–76, 77–82, 82–88, 88–98.

(13) Raw, C. J. G.; Frierdich, J.; Perrino, F.; Jex, G. *J. Phys. Chem.* **1978**, *82*, 1952–1953.

(14) Degn, H. European Molecular Biology Organization workshop, Dortmund, Oct 1976.

Laser and Pulse Radiolytically Induced Colloidal Gold Formation in Water and in Water-in-Oil Microemulsions

Kazue Kurihara,[1] Jerzy Kizling,[2] Per Stenius,[2] and Janos H. Fendler*[1]

Contribution from The Swedish Institue for Surface Chemistry, Drottning Kristinas vag 45, S-114 28, Stockholm, Sweden, and Clarkson College of Technology, Potsdam, New York 13676. *Received August 13, 1982*

Abstract: Reduction of $HAuCl_4$ has been investigated pulse radiolytically in water and in water-in-oil microemulsions. Rate constants have been determined for $Au^{3+} + e_{aq}^- \rightarrow Au^{2+}$, $2Au^{2+} \rightarrow Au^{3+} + Au^+$, and $Au^+ + R^-\cdot \rightarrow Au^0 + R$ (where $R^-\cdot$ is an unidentified radical). On the longer time scale formation of colloidal gold, $nAu^0 \rightarrow (Au^0)_n$, has been observed. Rate of colloidal gold formation has also been studied in the bombardment of $HAuCl_4$ solutions by 353-nm 60-mJ 3–5-ns laser pulses. Hydrodynamic diameters and polydispersities of empty and colloidal-gold-containing microemulsions have been determined by dynamic laser light scattering to be 150 and 220 Å, respectively. Morphologies of colloidal gold have been determined by electron micrography. There are a number of advantages of forming colloidal particles in microemulsions. Under identical conditions a greater amount of colloidal particles is formed than that in water. Colloidal gold particles formed in microemulsions are smaller and more uniform than those obtained in homogeneous solutions.

Introduction

Colloidal gold formation has been recognized for over 80 years.[3-5] Most methods of preparation involved the controlled chemical reduction of chloroauric acid, $HAuCl_4$. The size of the particles (typically between 100 and 600 Å) and their distribution,

(1) Clarkson College of Technology.
(2) Institute for Surface Chemistry, Stockholm, Sweden.

(3) "Gmelins Handbuch der Anorganischen Chemie"; Verlag Chemie: GmbH, Weinheim/Bergstr., Germany, 1975; Vol. 62, Appendix 3, p 183.
(4) Papavassiliou, G. C. *Prog. Solid State Chem.* **1979**, *12*, 185.

0002-7863/83/1505-2574$01.50/0

Table I. Dynamic Laser Light Scattering of PEGDE Microemulsions in the Absence and in the Presence of Colloidal Gold[a]

system	θ, deg[b]	diameter, Å[c]	Q[d]
PEGDE microemulsion[e]	90	142	0.033
	45	152	0.179
	60	142	0.178
	135	248	0.368
colloidal gold in	90	223	0.274
PEGDE microemulsion	60	267	0.503
	120	216	0.700
	135	208	0.650

[a] Obtained at 25 °C. There is a pronounced dependence of microemulsion morphologies on temperature (J. Kizling and P. Stenius, unpublished results). [b] θ = scattering angle. [c] Diameter $R_d = k_B T q^2/3\pi\eta\Gamma$, where k_B = Boltzmann constant, T = absolute temperature of sample, 298 K, η = viscosity of solvent (*n*-hexane), $q = 4\pi n/\lambda \sin(\theta/2)$ (λ = excitation wavelength = 488 nm, n = 1.372). [d] Q is the ratio of the second-order coefficient to the first-order coefficient squared ($Q = \mu^2/\bar{\Gamma}^2$) and is indicative of polydispersity. (The higher the Q the more polydisperse the system). Q values of 0.2 or less indicate a high degree of monodispersity. [e] See Experimental Section for composition.

growth rates, and stabilities depended markedly on the method of preparation and on the presence of stabilizers.[5] The possibility of using colloidal silver[6-11] and gold[12,13] as condensors for electron storage in artificial photosynthesis has prompted the recent renewed interest in these areas.

Reduction of chloroauric acid, $HAuCl_4$, by hydrated electrons, generated in pulse radiolysis, or by 353-nm laser pulses and the observation of colloidal gold formation in water and in microemulsions are the subject of the present report. Microemulsions provide good media for the preparation of relatively monodisperse small stable colloidal metal dispersions that, among other applications, can be used as catalysts.[15-18] Particularly noteworthy is the formation of monodisperse 30–50-Å diameter Pt, Pd, Rd, and Ir particles, which can be transferred to solid support without agglomeration.[16] Monodisperse Ni and Fe borohydride particles of high catalytic activity have also been prepared in reversed micelles.[17,18] Our interest lies in the detailed characterization and exploitation of these systems.

Experimental Section

Pentaethylene glycol dodecyl ether, PEGDE, was prepared by molecular distillation of the commercial surfactant Berol 050, which according to the manufacturer (Berol, Stenungsund, Sweden) has a distribution of chain lengths with a mean value of 5 units in the POE chain. The main impurities are dodecanol and sodium chloride. Low-boiling impurities were removed by six consecutive distillations at 10^{-3} mmHg and 50, 70, 80, 90, 100, and 115 °C, respectively. The residue of the last distillation was finally distilled at 10^{-3} mmHg and 125 °C, and the distillate was used as the final product. $HAuCl_4$ (Fluka), and spectra grade *n*-hexane (MCB) were used as received. Water was triple distilled.

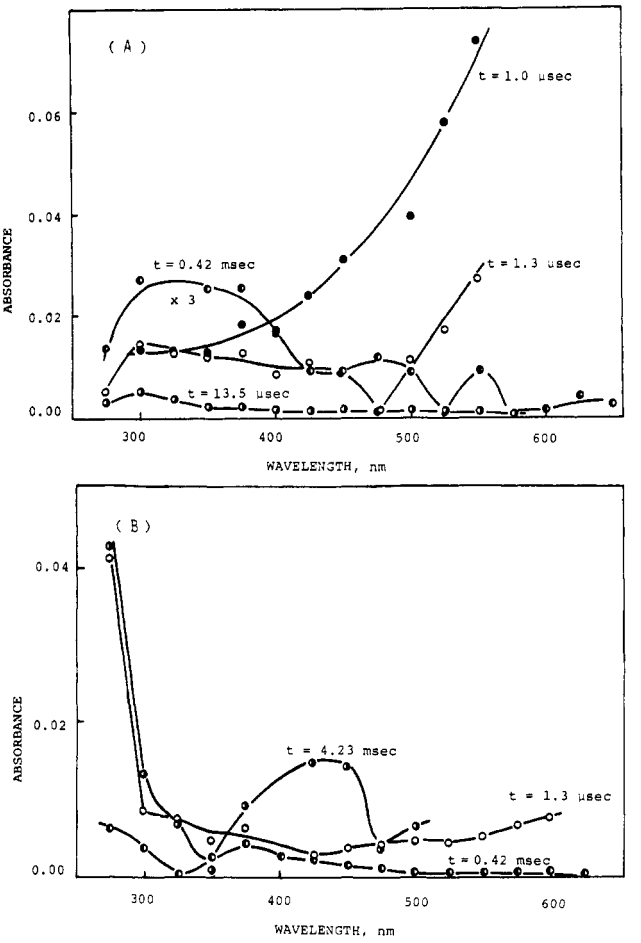

Figure 1. Transient absorption spectra of the pulse radiolytically formed species in degassed 2.0×10^{-4} M $HAuCl_4$ solutions at pH 8.0 (NaOH) containing 0.1 M MeOH in water (A) and in PEGDE microemulsions (B).

Microemulsions were prepared by adding water to appropriate concentrations of PEGDE in *n*-hexane to give 5:1:44 (w/w) ratios of PEGDE:H_2O:*n*-hexane. $HAuCl_4$ solutions were prepared by adding required amounts of 0.29 M aqueous $HAuCl_4$ stock solutions to water or microemulsions. Stoichiometric $HAuCl_4$ concentrations were $\sim 2 \times 10^{-4}$ M. Samples were deoxygenated by Ar or N_2 bubbling.

Pulse radiolysis experiments were carried out at the Center for Fast Kinetics Research, Austin, TX. Typical pulse widths were 400 ns and pulse doses were between 0.5 and 3.5 krd.[19] Laser photolysis experiments were carried out with a Quanta-Ray DCR Nd:Yag laser by using the third harmonic (353 nm) line, set to deliver 60-mJ/pulse of 5 ns width at 10-Hz repetition rate for photolysis, while single pulses along with the detection system were used for kinetic measurements.[20]

Particle sizes of the gold colloids were determined by transmission electron microscopy with a Philips EM 300G microscope. The maximum resolution of this microscope is ≈0.5 nm. Particles were directly deposited on a grid without extensive aggregation by evaporation of the solvent from a drop of solution on the support.

Hydrodynamic measurements were taken on a Malvern 2000 light-scattering system equipped with a Spectra Physics 171 argon ion laser, a digital correlator, microcomputer, and refractive index matched optical specimen cell assembly. Absorption spectra were taken on a Cary 118C spectrophotometer.

Results and Discussion

Dynamic Laser Light Scattering Measurements. Table I collects data for the hydrodynamic measurements for PEGDE micro-

(5) Turkevich, J.; Stevenson, P. L.; Hillier, J. *Discuss. Faraday Soc.* **1951** *11*, 55.
(6) Henglein, A.; Proske, Th. *Ber. Bunsenges. Phys. Chem.* **1978**, *82*, 471.
(7) Henglein, A. *Ber. Bunsenges. Phys. Chem.* **1980**, *84*, 253.
(8) Henglein, A. *J. Phys. Chem.* **1980**, *84*, 3461.
(9) Henglein, A.; Tausch-Treml, R. J. *Colloid Interface Sci.* **1981**, *80*, 84.
(10) Henglein, A.; Lillie, J. *J. Am. Chem. Soc.* **1981**, *103*, 1059.
(11) Jao, T. C.; Beddard, G. S.; Tundo, O.; Fendler, J. H. *J. Phys. Chem.* **1981**, *85*, 1963.
(12) Meisel, D. *J. Am. Chem. Soc.* **1979**, *101*, 6133.
(13) Westerhausen, J.; Henglein, A.; Lillie, J. *Ber. Bunsenges. Phys. Chem.* **1981**, *85*, 181.
(14) Gerischer, H.; Katz, J. J. "Light Included Charge Separation in Biology and Chemistry"; Verlag Chemie: New York, 1979. Claesson, S.; Engstrom, M. "Solar Energy—Photochemical Conversion and Storage"; National Swedish Board for Energy Conversion and Storage: Stockholm, Sweden, 1977. Gratzel, M. *Acc. Chem. Res.* **1981**, *14*, 376. Calvin, M. *Ibid.* **1978**, *11*, 4701.
(15) Boutonnet, M.; Anderson, C.; Carsson, R. *Acta Chem. Scand., Ser. A* **1980**, *A34*, 639.
(16) Boutonnet, M.; Kizling, J.; Stenius, P.; Maire, G. *Colloids Surf.*, in press.
(17) Nagy, J. B.; Gourgue, A.; Deroune, E. G. *Stud. Surf. Sci. Catal.* **1982**. Preparation of Catalysts. Third International Symposium on Scientific Bases for the Preparation of Heterogeneous Catalysts"; Louvan-la-Neuve, Sept 1982; Elsevier:Amsterdam, 1982.
(18) Lufimpadio, N.; Nagy, J. B.; Deroune, E. G. Proceedings of the Symposium on Surfactants in Solution, Lund, Sweden, June 1982.
(19) Lindig, B. A.; Rodgers, M. A. J. *J. Phys. Chem.* **1979**, *83*, 1683.
(20) Escabi-Perez, V. C.; Beddard, G. S.; Fendler, J. H. *J. Phys. Chem.* **1981**, *85*, 2316.

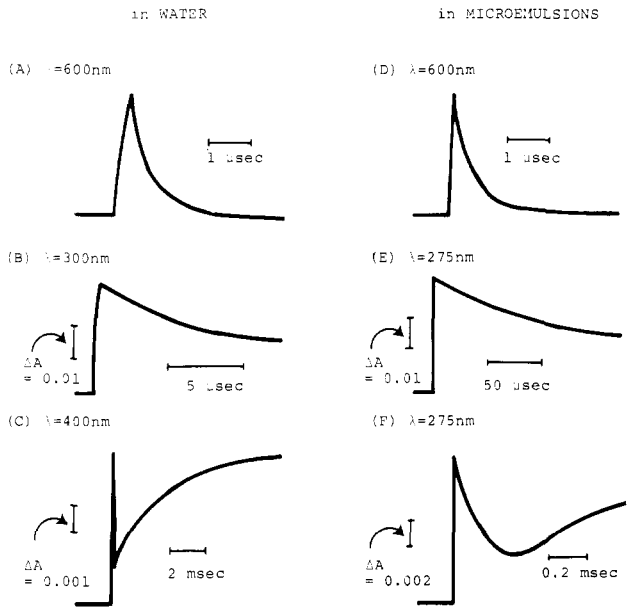

Figure 2. Time course of transient absorptions at various wavelengths in water and in PEGDE microemulsions.

emulsions in the absence and in the presence of colloidal gold. Hydrodynamic diameters are in the expected range,[21] and the microemulsions show quite remarkable degree of monodispersity. The second half of Table I shows the diameters of particles in the colloidal dispersions subsequent to the formation of colloidal gold. These particles are substantially larger and more polydisperse than the empty microemulsions.

Pulse Radiolysis of $HAuCl_4$ in Water and in Microemulsions. Hydrated electrons were generated in aqueous solutions and in surfactant-entrapped water pools[22-24] by a single pulse of 3-MeV electrons delivered by a Van de Graaf generator:[25]

$$H_2O \rightsquigarrow e_{aq}^- + \cdot H + \cdot OH + H_2O_2 + H_2 + H_3O^+ \quad (1)$$

In water, addition of 0.1 M methanol ensured the scavenging of the ·OH and ·H:

$$CH_3OH + \cdot OH \rightarrow \cdot CH_2OH + H_2O \quad (2)$$

$$CH_3OH + \cdot H \rightarrow \cdot CH_2OH + H_2 \quad (3)$$

In microemulsions, the rate constants of ·H and ·OH with the surfactant is sufficiently high to ensure the scavenging of these species.[25] Conversely, surfactants react **4–5** orders of magnitude slower with e_{aq}^- than with ·H or ·OH.[25]

Figure 1 shows the transient spectra of the species present subsequent to energy deposition in $HAuCl_4$ solutions of water and microemulsions. The absorbance around 600 nm is ascribed to e_{aq}^-. The decay of this absorbance, with half-life times of 3.26×10^{-7} s in water and 2.57×10^{-7} s in microemulsions, led to the buildup of a new absorbance with maximum at 300 nm in water and 270 nm in the microemulsion. The transient absorbing at 300 nm is due to Au^{2+},[26] formed in

$$Au^{3+} + e_{aq}^- \xrightarrow{k_4} Au^{2+} \quad (4)$$

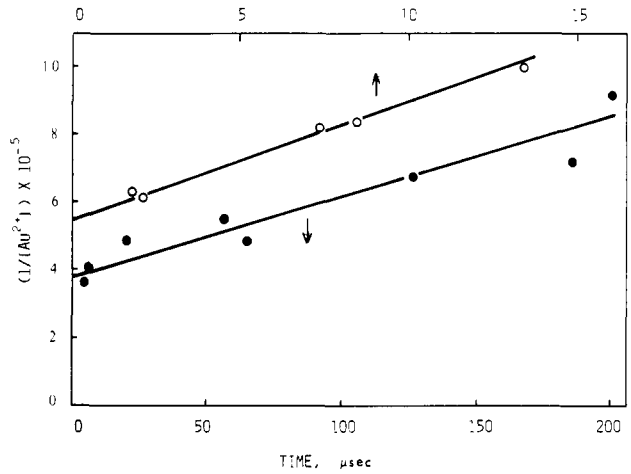

Figure 3. Disproportionation of Au^{2+}: second-order plots of the absorbances at 300 nm in water (○) and those at 275 nm in microemulsions (●) as functions of time.

Table II. Kinetic Data for Au^{3+} Reduction in Water and in Water-in-Oil Microemulsions

	water	microemulsion
half-life time of e_{aq}^-,[a] s	3.26×10^{-7}	2.57×10^{-7}
e_{aq}^- produced,[a] M	1.7×10^{-6}	2.4×10^{-6}
Au^{2+} produced, M	1.8×10^{-6}	2.6×10^{-6}
k_5, M^{-1} s^{-1}	3.6×10^{10}	2.1×10^{9}
$k_6[R\cdot]$, s^{-1}	2.8×10^{2}	1.16×10^{4}

[a] The extinction coefficient of e_{aq}^- at 600 nm was assumed to be 10^4 M^{-1} cm^{-1}; no correction has been made for the slight difference (±10%) in the absorbed electron dose.

Subsequent to its buildup the absorption due to Au^{2+} decreases, albeit comparatively slowly, by second-order kinetics (Figure 2). This process is due to the disproportionation of divalent gold cation:

$$2Au^{2+} \xrightarrow{k_5} Au^{3+} + Au^+ \quad (5)$$

Taking the extinction coefficient of Au^{2+} at absorption maximum wavelength to be 5.8×10^3 M^{-1} cm^{-1},[26] concentrations of initially produced Au^{2+} in water and in the microemulsions were determined to be 1.9×10^{-6} M and 2.6×10^{-6} M, respectively, from the intercepts of the plots shown in Figure 3. Similarly, using this extinction coefficient rate constant for reaction 5, k_5 has been calculated to be 3.6×10^{10} M^{-1} s^{-1} in water and 2.1×10^9 M^{-1} s^{-1} in microemulsions. Table II summarizes data for Au^{3+} reduction in water and in water-in-oil microemulsions. Disproportionation of Au^{2+} in microemulsions are limited by the exchange of the water pools between individual microemulsion droplets.[21] The smaller value for k_5 in microemulsions than that in water is a reflection of this process (see below).

The Au^+ formed (not identified in the transient spectra) in the disproportion of Au^{2+} (reaction 5) reacts with R· in a pseudo-first-order process to yield a long-lived species, having an absorption maximum at 350 nm in water and at 425 nm in microemulsions (Figures 1 and 2). This reaction is attributed to[26]

$$Au^+ + R\cdot \xrightarrow{k_6} Au^0 \quad (6)$$

where R· is an unidentified reducing species. Apparent first-order rate constants for reaction 6 ($k_6[R\cdot]$) were calculated to be 2.8×10^2 and 1.16×10^4 s^{-1} in water and in the microemulsion, respectively. The faster rate in microemulsions is related to the higher effective concentration of radicals in this environment than in water.

On a time scale slower than observable in pulse radiolysis a stable absorbance, with a broad maximum centered around 530 nm, developed. This process is the consequence of colloidal gold formation:

$$nAu^0 \rightarrow (Au^0)_n \quad (7)$$

(21) Eicke, H. F. *Top. Curr. Chem.* **1980**, *87*, 85. Zulauf, M., Eicke, H. F. *J. Phys. Chem.* **1979**, *83*, 408. Robinson, B. IVth ESF Workshop on Polymer Sciences, "Biological and Technological Relevance of Reversed Micelles and Other Amphiphilic Structures in Apolar Media"; Rigi-Kaltbad: Switzerland, Sept 1982.

(22) Wong, M.; Gratzel, M.; Thomas, J. K. *Chem. Phys. Lett.* **1975**, *30*, 329.

(23) Thomas, J. K.; Grieser, F.; Wong, M. *Ber. Bunsenges. Phys. Chem.* **1978**, *82*, 937.

(24) Fendler, J. H.; Fendler, E. J. *Prog. Phys. Org. Chem.* **1970**, *7*, 229.

(25) Fendler, J. H.; Bogan, G. W.; Fendler, E. J.; Infante, G. A.; Jirathana, P. In "Reaction Kinetics in Micelles"; Cordes, E. H., Ed.; Plenum Press: New York, 1973; p 53.

(26) Ghosh-Mazumder, A. S.; Hart, E. J. *Adv. Chem. Ser.* **1968**, *81*, 193.

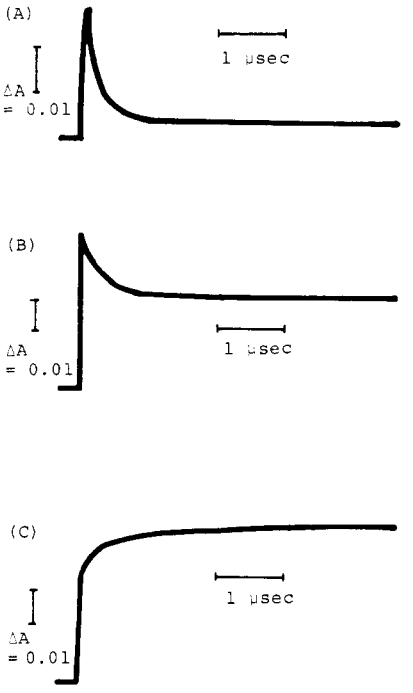

Figure 4. Transient absorbances observed at 525 nm in degassed 2×10^{-4} M $HAuCl_4$ in PEGDE microemulsions subsequent to excitation by 353-nm laser pulses. The time dependences are shown subsequent to exposure to two (A), ten (B), and several hundred (C) laser shots.

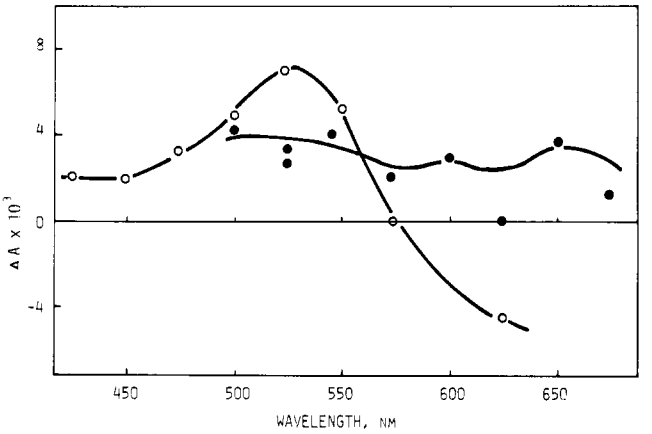

Figure 5. Transient spectra subsequent to laser irradiation of 2.0×10^{-4} M $HAuCl_4$ in PEGDE microemulsions subsequent to exposure to less than 30 (●) and several hundred (○) laser pulses.

Laser Photolysis of $HAuCl_4$ in Water and in Microemulsions. Excitation of $HAuCl_4$ solutions by energetic laser pulses resulted in irreversible spectral changes. The outcome of laser photolysis depended very much on the exposure time. In samples not exposed to more than three to six 5-ns 60-mJ pulses, only transients ($\tau \leq 1$ ms) were observable. Repeated (>10 shots) bombardment led to longer and longer lived species, which ultimately (>50 shots) became stable products. Figure 4 illustrates a typical behavior of transients at 525 nm. The outcome of flash photolysis was also found to depend on the time interval between consecutive shots. Under these conditions, the obtained transient spectra can be discussed only qualitatively.

Excitation of $HAuCl_4$ solutions unexposed to prior pulsing caused the bleaching of the ground-state absorbance in the submicrosecond time scale and the concomitant buildup and decay of transients with broad absorbance in the 400–600-nm region (Figure 5). Subsequent pulsing of the same solution resulted in the buildup of longer lived transients absorbing in the 550-nm region (Figure 5). Bombardment of $HAuCl_4$ solutions at 10 Hz for 30 s or longer led to the buildup of stable photoproducts whose absorbances were measured in the Cary spectrophotometer (Figure 6). These results can be discussed, tentatively, in terms of the formation of a caged divalent gold complex (eq 9) following excitation (eq 8). The complex then dissociates (eq 10) and

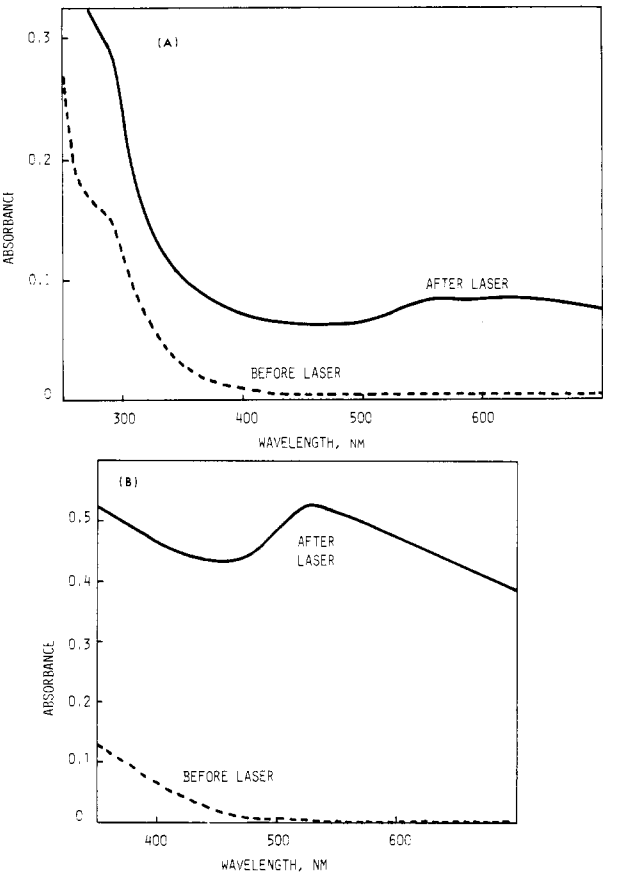

Figure 6. Development of colloidal gold subsequent to bombardment of 2.0×10^{-4} M $HAuCl_4$ solutions by 353-nm 60-mJ 10-Hz laser pulses for 5 min in water (A) and for 1 min in microemulsions (B).

$$(HAu^{3+}Cl_4) \xrightarrow{h\nu} (HAu^{3+}Cl_4)^* \quad (8)$$

$$(HAu^{3+}Cl_4)^* \rightarrow (HAu^{2+}Cl_3 \cdots Cl) \quad (9)$$

$$(HAu^{2+}Cl_3 \cdots Cl) \rightarrow HAu^{2+}Cl_3 + Cl \quad (10)$$

$$HAu^{2+}Cl_3 \rightarrow HAu^{3+}Cl_4 + HAu^{+}Cl_2 \quad (11)$$

$$HAu^{+}Cl_2 \xrightarrow{h\nu} Au^0 + HCl + Cl \quad (12)$$

$$nAu^0 \rightarrow (Au^0)_n \quad (7)$$

disproportionates (eq 11). Similar spectra have been previously reported for divalent gold charge-transfer complexes.[26] The long term buildup of stable absorbance is due, of course, to colloidal gold formation (eq 7), subsequent to the reduction of the gold monocation (eq 12). The dependency of the evolution of the transient absorption spectra on exposure time (Figure 5) suggests that the Au^{3+} reduction to Au^0 is a multiphoton event. Complexity of this spectrum precludes, however, more detailed mechanistic assignments.

Importantly, there is considerable more colloidal gold produced in microemulsions than in water under identical amounts of laser exposure (Figure 6). The colloidal gold formed in laser excitation remained stable for days. Once again those in microemulsions showed somewhat longer stabilities.

Kinetics of Colloidal Gold Formation. Subsequent to bombardment with 10-Hz 5-ns 60-mJ laser pulses there was a relatively slow development of stable absorbances due to colloidal gold formation (eq 7). Figure 7, A and B, illustrates the time dependence of this process in water and microemulsions, respectively. Several important differences between colloidal gold formation in the two systems merit qualitative discussions.

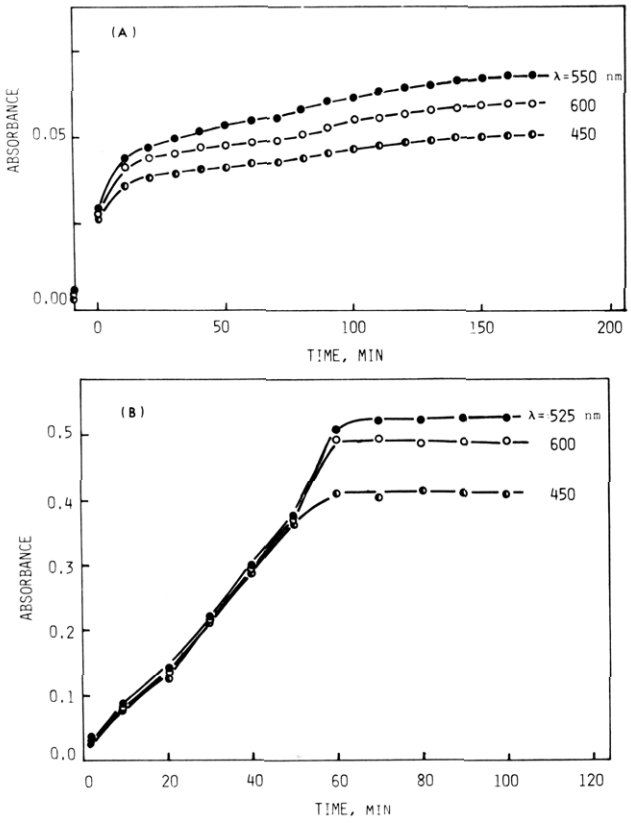

Figure 7. Buildup of colloidal gold (in the dark) subsequent to exposure of 2.0×10^{-4} M $HAuCl_4$ solutions to 353-nm 60-mJ 10-Hz laser pulses in water for 5 min (A) and in PEGDE microemulsions for 1 min (B).

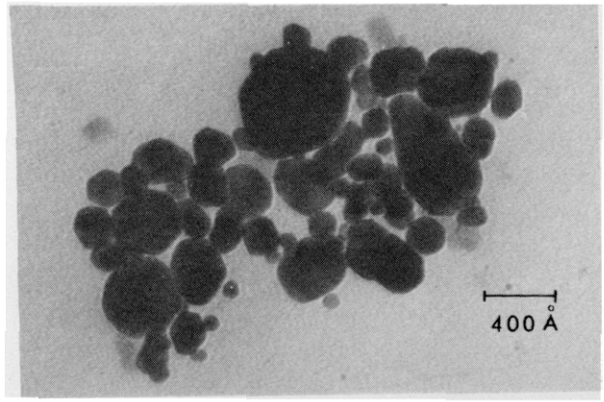

Figure 8. Electron micrograph of gold colloid particles formed in water.

Absorbances of colloidal gold formed in microemulsion was approximately 5 times greater than that in water even though the aqueous solutions received 5-fold more laser doses than the microemulsions (compare Figure 6, parts A and B). In aqueous $HAuCl_4$ solutions, unlike in microemulsions, colloidal gold formation was barely observable subsequent to exposure to laser pulses for 1 min. Since the extinction coefficient of colloidal gold increases with increasing particle size,[28] the higher absorbance in microemulsions (at ca. 150-Å gold particle diameter) than that in water (at ca. 400-Å gold particle diameter) implies the formation of higher concentrations of colloidal gold in microemulsions. Colloidal gold formation is apparently a less efficient process in bulk than in surfactant-entrapped water pools. Further, in microemulsions the absorption of colloidal gold, formed either in pulse radiolysis or in laser photolysis (Figure 6), has a pronounced maximum at 525 nm. Conversely, in water and absorption spectrum of colloidal gold is broader, is shifted to longer wavelength, and may be resolved into two maxima. These observations are explicable in terms of the formation of larger colloidal gold particles in water than in microemulsions.[27] Recently calculated

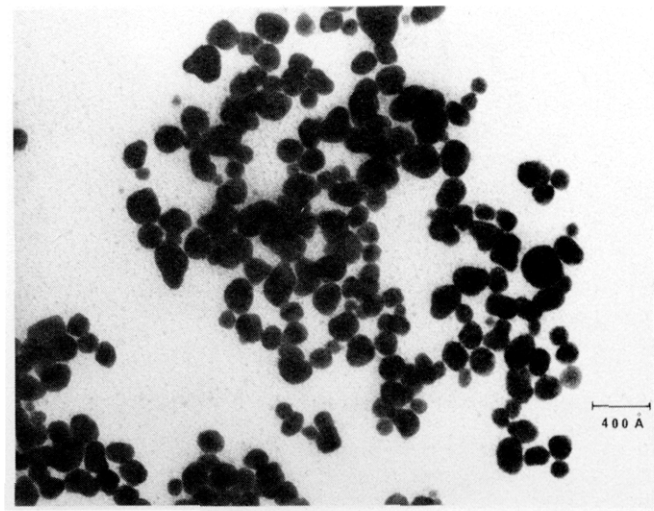

Figure 9. Electron micrograph of gold colloid particles formed in PEGDE microemulsion.

extinction cross sections for gold particles of 25–100-Å diameter indicated absorption maxima at 525 nm.[28] Absorption maxima for particles with diameters of 150, 250, and 350 Å shifted to 540, 570, 640 nm, respectively.[28] On the basis of this calculation an upper limit of a 150-Å diameter can be placed on the mean sizes of colloidal gold in microemulsions. Rates of growth of colloidal gold are also different in the two media (compare parts A and B in Figure 7). In water the absorbance increase is relatively slow and gradual at all wavelengths. Conversely, in microemulsions absorbances at different wavelength increase at the same rate in the initial 50 min, after which the absorbances at 530 nm increase at a somewhat greater rate than those at shorter wavelength. It is interesting to observe that the growth of colloidal gold particles are orders of magnitude slower than that observed for corresponding silver particles.[9]

Electron Micrography. Figures 8 and 9 illustrate typical electron micrography obtained from colloidal gold samples, formed by laser photolysis in water and in PEGDE microemulsion. Particles in microemulsion are seen to be smaller, more uniform, and less agglomerated than those in water. The mean diameters of colloidal gold, determined from the electron micrographs, are ca. 150 Å in microemulsions and ca. 400 Å in water.

Role of Microemulsion. Taking the mean diameter of the microemulsion aggregates that contain dissolved $HAuCl_4$ to be 220 Å results in a 114-Å diameter for the surfactant-entrapped water pool. Further, at the surfactant concentrations used the concentration of microemulsions is 3.3×10^{-5} M. At the concentrations of $HAuCl_4$ used (2×10^{-4} M), each microemulsion contains, therefore, approximately six Au^{3+} ions.[29]

(27) Mie, C. *Ann. Phys.* **1980**, *25*, 377. Franstein, C. V.; Romer, H. *Z. Phys.* **1958**, *151*, 54.

(28) Blatchford, C. Thesis, University of Kent, U.K., 1981.

(29) At the composition of the microemulsions (*n*-hexane = 4.4 g, d_h = 0.67; PEGDE = 0.5 g, d_p = 0.8; H_2O = 0.1 g, d_w = 1), the weight of water w_w and the weight of surfactant phase w_s are given by $w_w = {}^4/_3\pi r_1{}^3 d_w$ and $w_s = {}^4/_3\pi(r_2{}^3 - r_1{}^3)d_p$, where r_1 and r_2 are the radius of the water pool and the microemulsion, respectively:

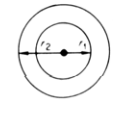

Taking r_2 = 110 Å (from light scattering data in Table I) allowed the calculation of r_1 from

$$\frac{w_w}{w_w} = \frac{0.1\text{ g}}{0.5\text{ g}} = \frac{{}^4/_3\pi r_1{}^3(1)}{{}^4/_3\pi(110^3 - r_1{}^3)0.8}$$

to be r_1 = 57 Å. Further, the weight of one microemulsion is $w_w + w_s = 4.6 \times 10^{-18}$ g, and hence the molecular weight of the microemulsion is 2.8×10^6 and its concentration is 3.3×10^{-5} M. There are therefore six Au^{3+} per microemulsion. It should be realized that these calculations are necessarily approximate.

Taking into consideration the efficiency of hydrated electron reactivity with Au^{3+} (eq 5) in the microemulsion, the Au^{2+} formed is estimated to be 2.6×10^{-6} M. Thus, each microemulsion droplet contains less than one molecule of Au^{2+}. Under this condition Au^{2+} disproportionation (reaction 5) primarily occurs through the exchange of the contents of neighboring microemulsions.[21] It has been shown in several studies on the self-diffusion coefficients of water in microemulsions[29] that the diffusion coefficient is about 1 order of magnitude less than that in pure water. Since dissolved Au^{2+} in the microemulsion can be expected to follow the water, the experimentally determined ratio of rate constants for reaction 5 (k_5) in the two solvent systems agrees fairly well with the calculated diffusion coefficient ratio.

The size of microemulsion droplet also limits the size of gold colloids if Poisson's distribution prevails. Since surfactant-entrapped water molecules exchange on the milisecond time scale,[30] formation of larger colloidal particles are possible by aggregation of neutral gold atoms from different droplets. Growth is ultimately limited by statistical considerations. The rate of reduction has been shown to affect profoundly the morphology and hence the catalytic efficiency of colloidal metal particles.[5] High-energy laser pulses on electrons provide means for controlling the rates of colloidal growth and hence open the door to systematic investigations. The role of microemulsions is to compartmentalize desired amounts of Au^{3+}. Kinetic confinements within a water pool facilitate nucleation and limit the growth of gold colloids. Formation of uniform well-separated particles is an additional advantage of preparing metal colloids in the restricted environments of surfactant aggregates. Indeed, information could be obtained on the arrangements of atoms by lattice-imaging techniques in colloidal gold particles prepared by reducing Au^{3+} ions in liposomes. Conversely, no atomic arrangement could be discerned in particles prepared in homogeneous solutions.[31] Organized assemblies provide, therefore, a means for the in-depth investigation of uniquely arranged subcolloidal particles. Extension of this principle to catalytically active colloids is the subject of our current attention.

Acknowledgment. Support of this work by the Department of Energy (J.H.F.) and the Swedish Natural Research Council (P.S.) are gratefully acknowledged. Pulse radiolysis experiments were carried out at the Center for Fast Kinetic Research, University of Texas, Austin, TX. This facility is supported by NIH Grant RR-00886 from the Biotechnology Branch of the Division of Research Resources and by the University of Texas. We appreciate the competent technical assistance of Wayne Reed.

Registry No. Au, 7440-57-5; $HAuCl_4$, 16903-35-8.

(30) Lindman, B.; Stilbs, P.; Mosely, M. E. *J. Colloid Interface Sci.* **1981**, *83*, 569.

(31) R. J. P. William, private communication, 1982.

Proton-Exchange Rates in Solid Tropolone As Measured via ^{13}C CP/MAS NMR†

Nikolaus M. Szeverenyi, Ad Bax, and Gary E. Maciel*

Contribution from the Department of Chemistry, Colorado State University, Fort Collins, Colorado 80523. *Received October 5, 1982*

Abstract: The rate of proton exchange is measured for solid tropolone in a new type of ^{13}C CP/MAS NMR experiment. The analysis of the ^{13}C NMR data in conjunction with previous X-ray results suggests that the exchange rate is determined by the reorientation of the molecule in the lattice, involving an energetically unfavorable "out-of-plane" rotation to restore proper lattice packing.

Introduction

There has been considerable interest in a class of molecules having hydrogen bonding with a double-well potential. One such molecule, tropolone (2-hydroxy-2,4,6-cycloheptatrien-1-one), has recently been shown by a two-dimensional (2-D) NMR experiment to interconvert between two equivalent structures in the solid state.[1] This exchange can be represented as shown in Figure 1. In this paper we wish to report measurements of the proton exchange rate as a function of temperature and describe the new nmr experiment by which these data were obtained.

When examined as a liquid above its melting temperature (50–51 °C) in an ordinary ^{13}C NMR experiment, tropolone gives four sharp resonance signals, as shown in Figure 2a. This spectrum reflects the rapid interconversion shown in Figure 1 and results in the averaging of resonance positions for carbons C-1 with C-2, C-3 with C-7, and C-4 with C-6. The solid-state ^{13}C NMR spectrum obtained at room temperature by the conventional cross polarization/magic angle spinning technique (CP/MAS),[2] however, does not display this averaging behavior. Each individual carbon type, e.g., the carbonyl, the hydroxyl-bearing carbon, etc., are seen as individual resonances (Figure 2b). Even as the temperature is increased in the solid-state experiment, the peak positions and line widths are found to be unaffected. In a similar experiment with the compound naphthazarine, Shiau et al. have observed ^{13}C CP/MAS NMR spectra for both the nonexchanging and the exchanging system at different temperatures.[3]

Examination of tropolone at 35 °C via a 2-D ^{13}C NMR experiment on the solid yields a mapping out of the exchange network and facilitates the assignment of chemical shifts. Figure 3 shows the contour plot for such an experiment. This experiment is described in detail in ref 1 and is analogous to that proposed by Jeener and co-workers[4] for mapping out chemical-exchange networks in liquid samples. Suter and Ernst[5] have also used the

† Presented in part at the 23rd Experimental NMR Conference, Madison, WI Apr 1982.

(1) N. M. Szeverenyi, M. J. Sullivan, and G. E. Maciel, *J. Magn. Reson.* **47**, 462 (1982).
(2) (a) A. Pines, M. G. Gibby, and J. S. Waugh, *J. Chem. Phys.*, **59**, 569 (1973). (b) J. Schaefer and E. O. Stejskal, *J. Am. Chem. Soc.*, **98**, 1031 (1976).
(3) W.-I. Shiau, E. N. Duesler, I. C. Paul, D. Y. Curtin, W. G. Blann, and C. A. Fyfe, *J. Am. Chem. Soc.*, **102**, 4546 (1980).
(4) J. Jeener, B. H. Meier, P. Bachmann, and R. R. Ernst, *J. Chem. Phys.*, **71**, 4546 (1979).
(5) D. Suter and R. R. Ernst, *Phys. Rev. B*, **25**, 6038 (1982).

0002-7863/83/1505-2579$01.50/0